

# A New Paradigm for Designing High-Fracture-Energy Steels

M.E. FINE, S. VAYNMAN, D. ISHEIM, Y.-W. CHUNG, S.P. BHAT, and C.H. HAHIN

The steels used for structural and other applications ideally should have both high strength and high toughness. Most high-strength steels contain substantial carbon content that gives poor weldability and toughness. A theoretical study is presented that was inspired by the early work of Weertman on the effect that single or clusters of solute atoms with slightly different atom sizes have on dislocation configurations in metals. This is of particular interest for metals with high Peierls stress. Misfit centers that are coherent and coplanar in body-centered cubic (bcc) metals can provide sufficient twisting of nearby screw dislocations to reduce the Peierls stress locally and to give improved dislocation mobility and hence better toughness at low temperatures. Therefore, the theory predicts that such nanoscale misfit centers in low-carbon steels can give both precipitation hardening and improved ductility and fracture toughness. To explore the validity of this theory, we measured the Charpy impact fracture energy as a function of temperature for a series of low-carbon Cu-precipitation-strengthened steels. Results show that an addition of 0.94 to 1.49 wt pct Cu and other accompanying elements results in steels with high Charpy impact energies down to cryogenic temperatures (198 K [−75 °C]) with no distinct ductile-to-brittle transition. The addition of 0.1 wt pct Ti results in an additional increase in impact toughness, with Charpy impact fracture energies ranging from 358 J (machine limit) at 248 K (−25 °C) to almost 200 J at 198 K (−75 °C). Extending this concept of using coherent and coplanar misfit centers to decrease the Peierls stress locally to other than bcc iron-based systems suggests an intriguing possibility of developing ductile hexagonal close-packed alloys and intermetallics.

DOI: 10.1007/s11661-010-0485-y

© The Minerals, Metals & Materials Society and ASM International 2010

## I. INTRODUCTION

ONE major goal in the development of steels for structural and other applications is increased strength without sacrificing ductility and toughness. Most high-strength steels are martensitic. The strength of martensitic steels increases with carbon content. A high carbon content, however, leads to poor weldability as a result of the formation of a brittle heat-affected zone adjacent to the weld. One can overcome this problem by using steels with a low carbon content and by enhancing the strength with precipitates. This was the basis for the development of HSLA-80 and HSLA-100 Cu-precipitation-strengthened steels,<sup>[1–6]</sup> which now are used in Naval applications, mining and dredging equipment, heavy-duty truck frames, and are beginning to be used in bridge applications. More recently, Cu-alloyed steels also are being studied as potential high-strength, high-formability steels.<sup>[7]</sup> Depending on the strength and toughness requirements for the specific application, Cu-precipitation-strengthened steels may be supplied

in various conditions, including as-rolled, as-rolled and aged, normalized and aged, or quenched and aged. All conditions take advantage of copper precipitation to achieve the combination of improved strength and toughness. The primary purpose of this study is to provide a new insight into the underlying mechanisms at play in achieving a high-impact fracture energy at low temperatures in Cu-bearing low-carbon steels.

It has been known since the 1930s that the addition of Cu to steels leads to precipitation strengthening.<sup>[8]</sup> Over the years, the topic has been studied extensively.<sup>[9–14]</sup> Figure 1, extracted from the studies of Lahiri *et al.*,<sup>[11]</sup> shows the results for a binary Fe-1.67 at. pct Cu. After solution treatment at 1273 K (1000 °C) and aging at 773 K (500 °C), the flow stress at 0.2 pct strain increases rapidly with little or no incubation time, but the change in Young's modulus seems to require an incubation period of approximately 30 minutes. The body-centered cubic (bcc) Cu-Fe precipitation thus seems to occur in two stages. The initial stage does not lead to a change in Young's modulus. The aging of Cu-containing steels occurs in stages, beginning first as Cu clustering in the matrix, followed by bcc Cu alloy precipitates, transitioning into the 9R structure, and finally face-centered-cubic Cu precipitates. Using field ion microscopy and atom probe, Goodman *et al.*<sup>[15]</sup> observed the formation of coherent, coplanar bcc Cu precipitates that contain a substantial amount of iron.

Using laser-enhanced atom probe (LEAP) tomography, we recently analyzed one of Lahiri's aged specimens corresponding to the peak-aged condition

M.E. FINE and Y.-W. CHUNG, Professors, and S. VAYNMAN and D. ISHEIM, Research Professors, are with the Department of Materials Science and Engineering, Northwestern University, Evanston, IL 60208. Contact e-mail: m-fine412@northwestern.edu S.P. BHAT, Principal Research Engineer, is with ArcelorMittal Global Research and Development, East Chicago, IN 46132. C.H. HAHIN, Bridge Engineer, is with the Illinois Department of Transportation, Springfield, IL 62764.

Manuscript submitted June 17, 2010.

Article published online October 5, 2010

(solutionized at 1273 K [1000 °C] and aged for 2 hours at 773 K [500 °C]). Figure 2 shows a tomographic image containing 550 precipitates in a cylindrical volume of  $460 \times 10^{-24} \text{ m}^3$ , giving a number density of  $(1.2 \pm 0.1) \times 10^{24}/\text{m}^3$ . These precipitates contain approximately 30 at. pct Fe in agreement with Goodman *et al.*<sup>[15]</sup> The average radius of these Cu-containing precipitates is  $(1.2 \pm 0.05) \text{ nm}$ . As shown in Figure 1, such nanosized Cu alloy clusters or precipitates markedly increase the strength of the base metal.

In addition to their effects on strength, these nanosized coherent-coplanar precipitates improve the mobility of screw dislocations at low temperatures, resulting in lower ductile-to-brittle transition temperatures and in higher fracture energies, as detailed by the theoretical analysis in the next section. This section is followed by the recent results of our research efforts on Cu-precipitation-strengthened low-carbon steels with high-impact fracture energies at cryogenic temperatures

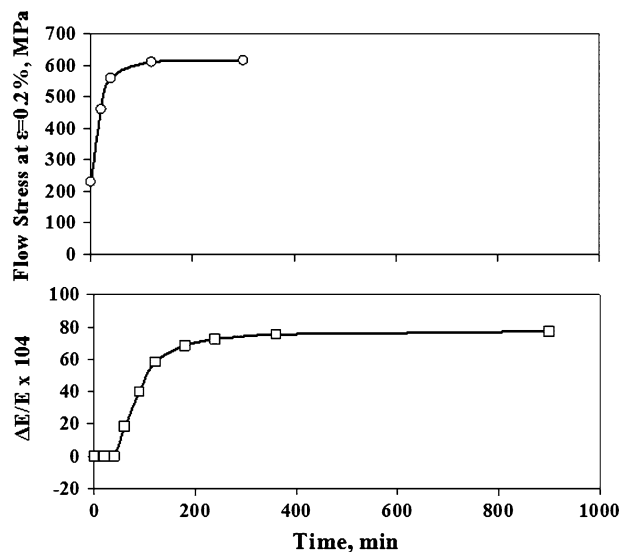


Fig. 1—Variation of flow stress at 0.2 pct offset strain as a function of aging time at 773 K (500 °C) for a binary Fe-1.67 at. pct Cu alloy. The alloy was subjected to solution treatment at 1273 K (1000 °C) before aging. The flow stress was measured at room temperature (after Lahiri *et al.*<sup>[11]</sup>).

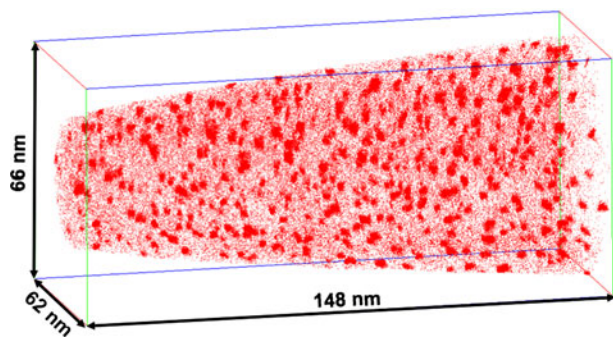


Fig. 2—Atom-probe tomographic analysis of nanoscale Cu alloy precipitates in Fe-1.67 at. pct Cu after 2 h of aging at 773 K (500 °C).

as well as a general discussion that includes the implications of this work for developing alloys and intermetallics that are more ductile.

## II. INTERACTION OF MISFIT CENTERS WITH HIGH PEIERLS STRESS DISLOCATIONS

The ductile-to-brittle transition in steels depends on the interplay between flow stress and fracture stress. In ferritic steels, the mobility of screw dislocations and consequently the flow stress depend strongly on temperature and strain rate. In contrast, the fracture stress usually is assumed to be independent of temperature and strain rate (this assumption neglects the minor temperature dependence of modulus<sup>[16]</sup> and its possible effect on fracture stress). At high temperatures (usually above room temperature) and low strain rates, thermal energy is sufficient to activate the motion of screw dislocations, resulting in plastic flow at stresses below the fracture stress. However, as one lowers the temperature, less thermal energy is available, and higher stress is required to activate the motion of screw dislocations. Therefore, the flow stress increases with decreasing temperature. Eventually, the flow stress curve intersects the fracture stress at a critical temperature, below which the steel suffers brittle fracture before yielding. This is the ductile-to-brittle transition temperature (DBTT) as shown in Figure 3. The DBTT increases with strain rate.

The stress (Peierls stress) to move a long dislocation segment from a crystallographic energy valley in bcc metals is large. Weertman proposed many years ago that a high Peierls energy dislocation likely would move by first forming a double kink<sup>[17]</sup> (Figure 4). In bcc metals, the kink sides are in an edge dislocation orientation and are thus very mobile. Subsequently, Weertman suggested that a solute atom (or clusters of solute atoms) misfit center would interact with a dislocation to help pull it from its Peierls energy valley<sup>[18]</sup> (Figure 5).

The plausibility of Weertman's idea is illustrated in the work of Dickensheid<sup>[19]</sup> on the variation of strain rate sensitivity with temperature for binary Fe-Ni alloys with different Ni concentrations (Figure 6). At high

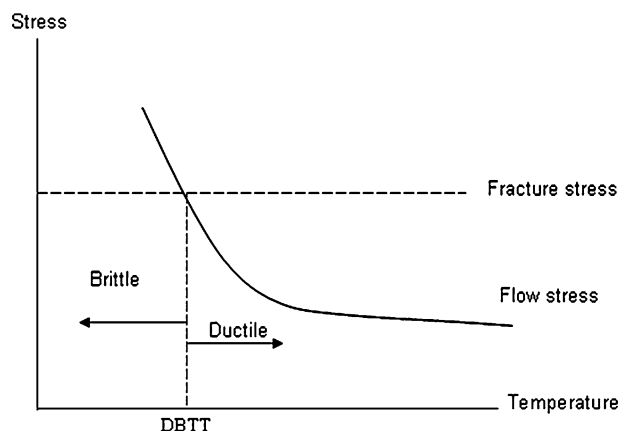


Fig. 3—Flow stress at constant strain rate vs temperature. The flow stress increases with decreasing temperature, eventually intersecting the fracture stress, thus resulting in ductile-to-brittle transition.

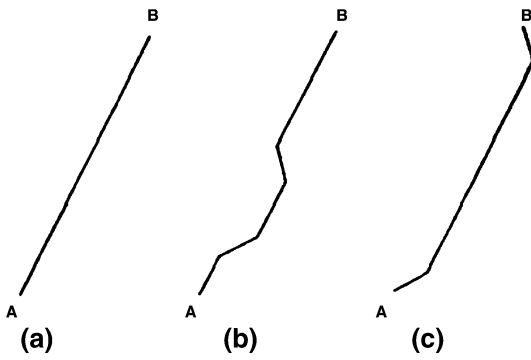


Fig. 4—Double-kink mechanism for moving a screw dislocation with high Peierls stress from one energy valley to the next (after Weertman<sup>[17]</sup>). (a) Original position of screw dislocation parallel to a Peierls valley. (b) Screw position after a jog is thrown over a Peierls hill into a neighboring valley (formation of double kink). (c) After expansion under stress of the double kink in (b).

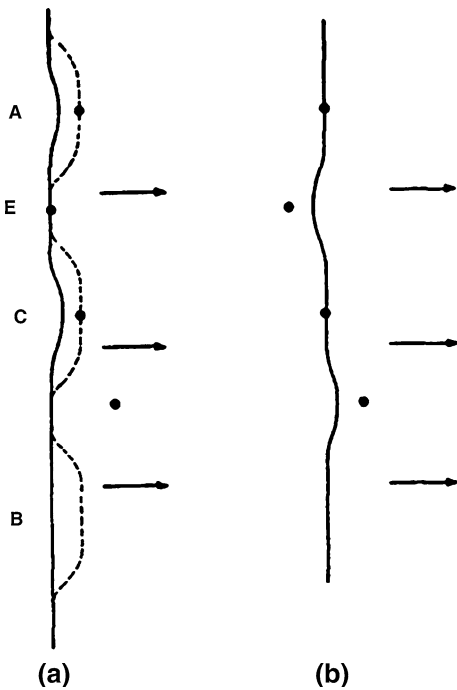


Fig. 5—Weertman's mechanism for the local reduction of Peierls stress caused by a nearby misfit center (after Weertman<sup>[18]</sup>). (a) Initial position. Formation of jogs (double kinks) at A and C (in the vicinity of misfit centers) requires less energy than at B, where no misfit centers are present. (b) After expansion of two double kinks formed at A and C.

temperatures, thermal energy is sufficiently large that the flow stress varies little with a strain rate over the range tested (from  $5 \times 10^{-4}/s$  to  $5 \times 10^{-3}/s$ ). On cooling, the decrease in thermal energy leads to an increase in strain rate sensitivity. At sufficiently low temperatures, thermal energy decreases to a low enough value to give little strain rate sensitivity of the flow stress. This type of behavior shows that a process is in play that requires activation energy. A peak value is observed at an intermediate temperature and then shifts to a lower temperature as the Ni content is increased, suggesting

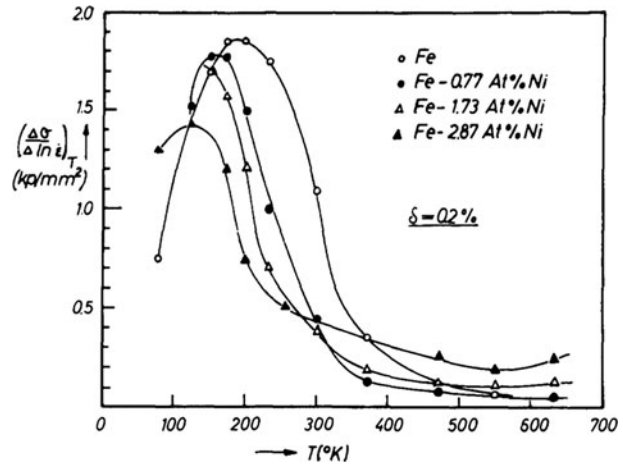


Fig. 6—Strain rate sensitivity of flow stress as a function of temperature for several binary Fe-Ni alloys (after Dickensheid<sup>[19]</sup>).

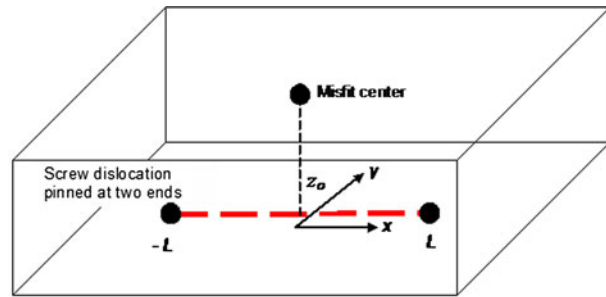


Fig. 7—A screw dislocation segment pinned at both ends in the vicinity of a misfit center (distance  $z_0$  above).

that the activation energy for plastic flow decreases as Ni is added to the ferrite. The authors suggest that Ni atoms, for example, are present in solution in bcc Fe form clusters analogous to an early stage of coherent coplanar precipitation.

Urakami and Fine<sup>[20]</sup> developed a mathematical treatment of the effect of a solute atom or solute cluster misfit center on a nearby dislocation segment pinned at both ends in the spirit of Weertman's idea. Their treatment is presented here in detail, using the geometry shown in Figure 7.

The energy  $I$  of the screw dislocation in the presence of a misfit center is expressed as follows:

$$I = \int \left[ E(y) \sqrt{1 + \left( \frac{dy}{dx} \right)^2} - \int_0^y F(x, s) ds \right] dx \quad [1]$$

where  $E(y)$  is the periodic Peierls potential energy per unit length of the screw dislocation, and  $F$  is the force of the misfit center acting on unit length of the screw dislocation. This integral is minimized when the integrand  $L$  (expression inside the square bracket) satisfies the following Euler-Lagrange equation:

$$\frac{\partial}{\partial x} \left( \frac{\partial L}{\partial p} \right) - \frac{\partial L}{\partial y} = 0 \quad \text{where } p = \frac{dy}{dx} \quad [2]$$

In this case,  $L = E(y)\sqrt{1 + \left(\frac{dy}{dx}\right)^2} - \int_0^y F(x, s)ds$  (i.e.,  $L$  is a function of  $x$ ,  $y(x)$ , and  $dy/dx$ ).

Direct computation reduces the Euler–Lagrange equation to the following:

$$E(y)\frac{dp}{dx}\frac{1}{(1+p^2)^{3/2}} - \frac{\partial E}{\partial y}\frac{1}{(1+p^2)^{1/2}} + F(x, y) = 0 \quad [3]$$

For simplicity, we will assume that the Peierls valleys vary with a period equal to the Burgers vector  $\mathbf{b}$  as follows:

$$E(y) = E_0 - A \cos\left(\frac{2\pi y}{\mathbf{b}}\right) \quad [4]$$

The term  $F(x, y)$ , the force acting on a unit length of the dislocation resulting from the misfit center, is expressed as follows:

$$F(x, y) = \frac{6\mu\mathbf{b}\varepsilon Vz_0x}{(x^2 + y^2 + z^2)^{5/2}} \quad [5]$$

where  $\mu$  is the shear modulus,  $\mathbf{b}$  is the Burgers vector,  $\varepsilon$  is the misfit strain,  $V$  is the volume of the misfit center, and  $z_0$  is the position of the misfit center above the glide plane. To simplify, we will express everything in dimensionless quantities as follows:

$$E_R = \frac{E_0}{\mu\mathbf{b}^2} \quad A_R = \frac{A}{\mu\mathbf{b}^2} \quad S = \frac{V}{\mathbf{b}^3}$$

In addition, we will normalize lengths by the following Burgers vector:

$$L_R = \frac{L}{\mathbf{b}} \quad x_R = \frac{x}{\mathbf{b}} \quad y_R = \frac{y}{\mathbf{b}} \quad z_R = \frac{z_0}{\mathbf{b}}$$

Equation [3] becomes the following:

$$\begin{aligned} [E_R - A_R \cos(2\pi y_R)] \frac{1}{(1+p^2)^{3/2}} \frac{dp}{dx_R} \\ + \frac{1}{(1+p^2)^{1/2}} 2\pi A_R \sin(2\pi y_R) + \frac{6S z_R x_R}{(x_R^2 + y_R^2 + z_R^2)^{5/2}} = 0 \end{aligned} \quad [6]$$

Typically,  $0.2 < E_R < 1.0$  and  $10^{-6} < A_R < 10^{-3}$ . The Peierls stress is  $2\pi\mu A_R$ .

Equation [6] can be solved numerically for given input values of  $L_R$ ,  $E_R$ ,  $A_R$ ,  $z_R$ , and  $S$ . To illustrate, we will assume that the dislocation segment is pinned by obstacles spaced  $80\mathbf{b}$  apart. The misfit center is located at  $20\mathbf{b}$  above the middle of the dislocation segment. As a reference,  $S = 1.0$  corresponds approximately to a spherical precipitate with a radius equal to  $5\mathbf{b}$  and a misfit strain of 0.2 pct.  $E_R$  and  $A_R$  are set to 0.5 and  $5 \times 10^{-5}$ , respectively. The result is shown in Figure 8 for  $S = 0.5, 1.0$ , and  $2.0$ . In the absence of thermal energy and with a given sinusoidal Peierls potential, the stress to move the dislocation is a maximum at  $\mathbf{b}/4$  from the Peierls valley. Therefore, if the effect of the misfit center is large enough to twist the dislocation locally by  $\mathbf{b}/4$ , then the dislocation will move spontaneously to the

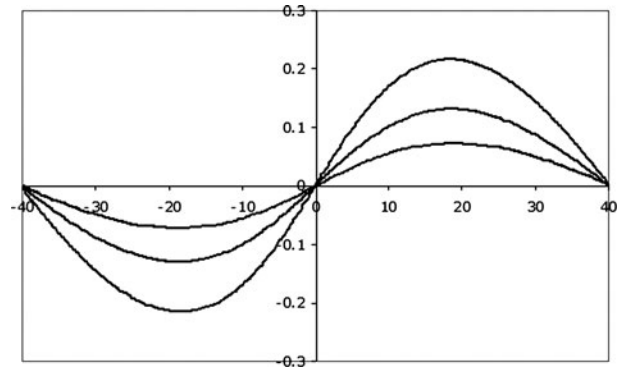


Fig. 8—Minimum energy configuration of a dislocation segment originally in screw orientation pinned by obstacles spaced  $80\mathbf{b}$  apart in the presence of a spherical misfit center located at  $20\mathbf{b}$  above the center of the dislocation segment (all units in Burgers vectors  $\mathbf{b}$ ). The input conditions are given in the text.

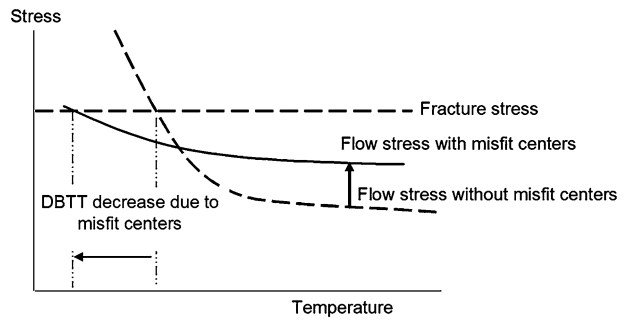


Fig. 9—Misfit centers strengthen the steel at elevated temperatures but reduce the flow stress at low temperatures, thereby lowering the DBTT.

next valley, forming a kink. As discussed earlier, the kink has an edge dislocation and sides have edge orientation. In bcc metals, they have a low Peierls energy, resulting in easy plastic flow. For the previous input conditions, the maximum twisting of the screw dislocation is between  $0.07$  and  $0.22\mathbf{b}$  as  $S$  varies from  $0.5$  to  $2.0$ . This is a significant fraction of  $\mathbf{b}/4$ . The Peierls stress needed for the screw segment to jump spontaneously into the next Peierls valley has been reduced.

The previous calculation demonstrates that a nearby misfit center indeed may provide sufficient twisting of a screw dislocation to reduce the activation energy for plastic flow. Except in dilute solid solutions, the misfit centers are unlikely to be single atoms. Clusters of solute atoms were thought<sup>[20,21]</sup> to be the bcc misfit centers causing solid-solution softening. In the current research, we suggest the nanoscale coherent and coplanar Cu alloy precipitates in a ferritic matrix act as misfit centers. In other words, the nanoscale precipitates seem to have dual roles; they increase the flow stress at room temperature because of precipitation strengthening, but they decrease the flow stress at low temperatures because of the interaction between stress fields of these misfit centers with nearby screw dislocations. As depicted in Figure 9, this interaction leads to a lower temperature dependence of flow stress and consequently to a lower DBTT. This opens a new paradigm for the



design of more ductile and more fracture-resistant steels, as well as a way to decrease the DBTTs in other bcc metals and related intermetallics.

### III. EXPERIMENTS AND RESULTS

In conjunction with the theoretical development given in Section II, a study of Charpy impact fracture energies of selected steels with coherent coplanar Cu alloy precipitates as a function of temperature was undertaken. The results reported in this study were obtained from the following Cu alloyed steels: (1) a commercial (80 ton) heat of American Society for Testing and Materials (ASTM) A710 grade B steel made by Oregon Steel Mills ((OSM) now Evraz), (2) a laboratory heat (45 kg) with 0.10 pct Ti prepared by U.S. Steel Research Center (USS), and (3) a reduced Cu and Ni alloy content 45 kg laboratory heat made by Sophisticated Alloys Inc. (SAI). The commercial heat was made in an electric furnace and was bottom poured. Both laboratory heats were made by vacuum induction melting. The steel alloys were hot rolled to thicknesses varying from 3 to 52 mm and then air-cooled. In this study, properties of only 12-mm-thick plates are presented. The chemical compositions are shown in Table I. The concentration of carbon was kept low. Nickel was added to the steel to prevent hot-shortness from Cu. The Ni-to-Cu ratio was maintained in the 0.5 to 0.7 range. Nb was added for grain refinement. Ti greater than a residual amount was introduced in the USS heat to tie up C and N. Standard tensile and Charpy specimens were machined in the rolling direction. Tensile testing was performed on an MTS screw-driven machine (MTS Systems Corporation, Eden Prairie, MN), and Charpy specimens were tested in a machine with a 358-J limit.

Table II summarizes the stress-strain curve mechanical properties of the three steels. All specimens tested were air-cooled from the final rolling temperature. The yield strengths and ultimate tensile strengths (UTSs) vary from 427 to 602 MPa and from 518 to 623 MPa, respectively, depending on the specific alloy compositions and the hot rolling practices used in the manufacture of these steels. All steels have good ductility with elongations to failure between 27 and 30 pct.

Noteworthy results of this study are the high values of Charpy impact fracture energy observed in these Cu-precipitation-hardened steels. Some specimens stopped the hammer and did not break in the Charpy apparatus. These specimens are marked with up-arrows in Figures 10, 11, and 13. Figure 10 shows Charpy impact fracture energy values for OSM ASTM A710B steel as a function of temperature down to 213 K (−60 °C). At room temperature and at 261 K (−12 °C), the specimens

did not fracture in the Charpy impact tests. Below this temperature, a gradual reduction was noted in the Charpy impact fracture energy. A lower shelf for impact fracture energy was not observed within the tested temperature range. Even at 213 K (−60 °C), the fracture is ductile and the Charpy impact fracture energy is approximately 190 J. This value is much greater than that usually associated with brittle fracture of steels below DBTT. For plain carbon steels, for example, the lower shelf impact fracture energy is in the 5 J to 20 J range.<sup>[22]</sup>

**Table II. Tensile Test Properties of the Three Cu Alloyed Steels, Air-Cooled from Hot Rolling**

Steel Heat	0.2 Pct Offset Yield Strength (MPa)	UTS (MPa)	Elongation to Failure (Pct)
OSM	602	623	27
USS	497	587	30
SAI	427	518	28

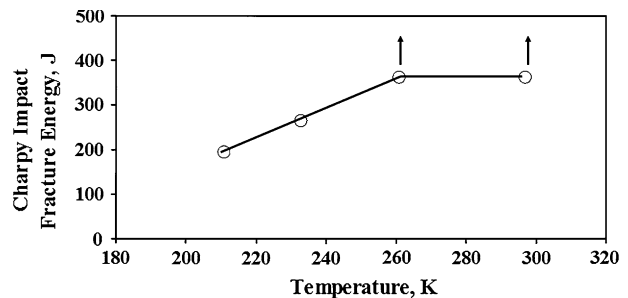


Fig. 10—Charpy impact fracture energy vs temperature for OSM steel. The arrows show specimens that broke partially and stopped the hammer, indicating that Charpy energy exceeds the 358-J limit of the machine.

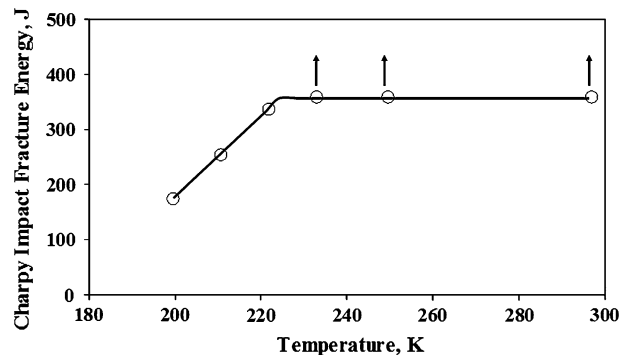


Fig. 11—Charpy impact fracture energy of USS steel containing 0.1 pct Ti vs temperature.

**Table I. Chemical Compositions (In Weight Percent) of Three Cu Precipitation Hardened Steels**

Steel Heat	Supplier	C	Cu	Ni	Mn	Si	Nb	Ti
OSM	Oregon Steel Mills	0.03	1.49	0.84	0.49	0.40	0.06	0.03
USS	USS Research Center	0.06	1.30	0.90	0.50	0.39	0.06	0.10
SAI	Sophisticated Alloys	0.07	0.94	0.49	0.87	0.30	0.07	0.03

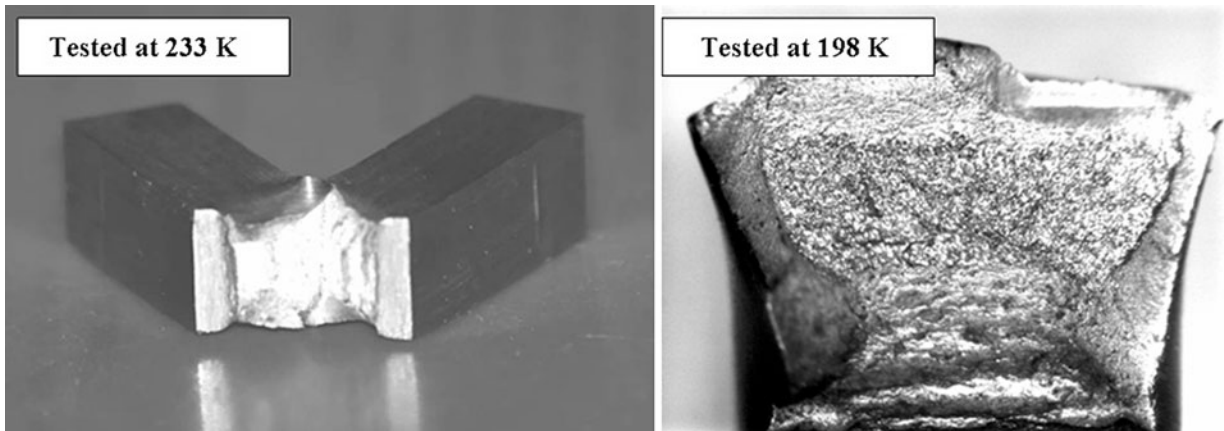


Fig. 12—Photographs of full-size Charpy specimens (10 mm × 10 mm) of USS steel after being tested at 233 K (−40 °C) and 198 K (−75 °C).

Figure 11 shows the variation of the Charpy impact fracture energy as a function of temperature for the steel labeled USS. It is evident that the addition of 0.1 wt pct Ti to tie up C and N interstitials improves the fracture toughness of the steel; although the OSM steel that contains 0.03 pct Ti does not fracture in the Charpy apparatus down to 261 K (−12 °C), the steel that contains 0.10 pct Ti does not fracture down to 233 K (−40 °C). Similar to OSM steel Charpy samples, no precipitous drop occurs in the Charpy impact fracture energy. Even at 198 K (−75 °C), the Charpy impact fracture energy for this steel is about 170 J, and a lower shelf was not reached.

Figures 12(a) and (b) show actual Charpy specimens of the USS Ti-modified A710B steel tested at 233 K (−40 °C) and at 198 K (−75 °C), respectively. Even at 198 K (−75 °C), the fracture is ductile during impact testing.

Figure 13 shows the variation of Charpy impact fracture energy as a function of temperature for the SAI steel. The steel contains 0.94 wt pct Cu, which is less than in the other two steels (1.3 to 1.49 Cu). The yield strength is in excess of 400 MPa. Three notable features are shown in Figure 13. First, the Charpy impact fracture energy exceeds by a large value the specifications for bridges (40 J in the 238 K to 253 K [−35 °C to −20 °C] temperature range). Second, even at the lowest test temperature of 198 K (−75 °C), the Charpy energy is still high (>90 J). Third, unlike the other two steels with higher Cu content, this steel shows a distinct ductile-to-less-ductile transition on cooling below 228 K (−45 °C), but the lower shelf value is high, approximately 100 J at 198 K (−75 °C).

#### IV. DISCUSSION

As presented in Section II, we demonstrate theoretically that coherent and coplanar misfit centers in bcc metals, such as enriched Cu clusters in the bcc matrix, can provide sufficient twisting of nearby screw dislocations to enhance their mobility in the absence of insufficient thermal activation. This twisting provides a

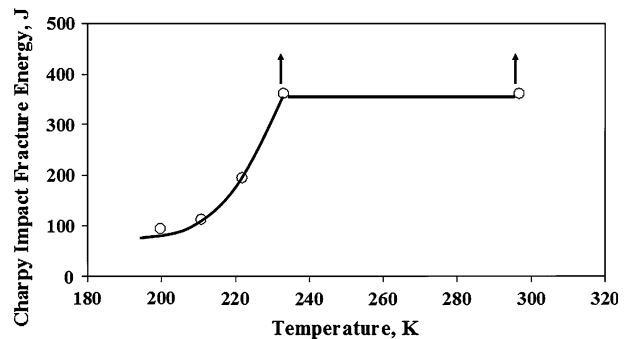


Fig. 13—Charpy impact fracture energy vs temperature for SAI (0.94 Cu) steel.

mechanism for ductilizing steel and for improving impact toughness at low temperatures. In this work, we have suggested that nanoscale Cu alloy bcc clusters/precipitates act as such misfit centers. An addition of 1.3 to 1.49 wt pct Cu with other accompanying elements results in steels with yield strength in the range of 500 to 600 MPa that may be suitable for many commercial applications requiring remarkably high fracture energy. The Charpy impact fracture energy data for these steels show that although the Charpy impact fracture energy decreases with temperature, it maintains remarkably high values (100 to 200 J) down to 198 K (−75 °C). The decrease is gradual with no indication of a sharp transition. The fracture surfaces are ductile, except sometimes for a small cleavage-like region adjacent to the center of the notch. This is not the type of fracture usually found in steels below the DBTT. When the Cu content is reduced to 0.94 wt pct, the yield strength decreases (slightly above 400 MPa) and is accompanied by a distinct ductile-to-less-ductile transition at 228 K (−45 °C), with a lower shelf energy of about 100 J. In usual steels, the DBTT is attributed to the thermally activated motion of screw dislocations, but the transition temperature is higher.

Although the origin of the high Charpy impact fracture energy at room and low temperatures is not fully understood, the authors attribute it to the

coherent, coplanar Cu alloy clusters/precipitates that are present. They play a role in ductilizing the low-temperature fracture process, as suggested by our theoretical analysis. The appearance of a ductile-to-less-ductile transition after reduction of the Cu content is consistent with this idea. The precipitation behavior observed in the model binary Fe-Cu alloy system in previous studies forms the basis of this discussion. Of course, other alloying elements<sup>[23]</sup> (e.g., Mn and Ni) and the specific temperature–time cycle the steel is subjected to are expected to influence greatly the kinetics and morphology of precipitates or clusters. All three steels used in the present study were air-cooled after hot rolling. Prior studies have demonstrated that nanoscale Cu precipitates form during continuous cooling. Auto-aging<sup>[24]</sup> and/or interface precipitation<sup>[25]</sup> have been suggested as the operating mechanisms. The results presented here seem to indicate that air-cooling after hot rolling leads to the needed fine precipitates and high-fracture energy steels without the necessity of added heat treatment. Additional studies are needed to confirm the structure and composition of Cu alloy precipitates in these air-cooled steels.

It is intriguing to propose that this concept can be extended to other materials in which a high Peierls stress limits the ductility. For example, hexagonal close-packed (hcp) metals such as Mg and Ti have a low Peierls stress for basal or prismatic slip, but the mobile dislocations have the same Burgers vector and not enough independent slip systems are available. Slip on pyramid planes is caused by dislocations with different Burgers vectors ( $c + a$  instead of  $a$ ), but high Peierls stress intervenes. Can nanoscale coherent, coplanar precipitates reduce the activation energy for pyramidal slip and make hcp metals more ductile at room temperature? Much interest is focused on intermetallics because of their low density and their excellent high-temperature strength, but their room-temperature ductility is limited because of high Peierls stress (they are ductile if the temperature is high enough). Again, can nanoscale coherent, coplanar precipitates locally lower the Peierls stress in intermetallics like NiAl? The concept presented in this study is suggested as a new tool for designing alloys with higher fracture energies and lower DBTTs.

## V. SUMMARY

Theory shows that misfit centers consisting of atom clusters in bcc metals can cause twisting of nearby screw dislocations. Such twisting can help to activate the motion of screw dislocations, thus resulting in improved dislocation mobility and fracture toughness at low temperatures. To explore the validity of this theory, we measured the Charpy impact fracture energy as a function of temperature for a series of low-carbon Cu alloy precipitation-strengthened steels. The findings show that an addition of 1.3 to 1.5 wt pct Cu and other accompanying elements results in steels with no distinct ductile-to-brittle transition, with excellent Charpy energies ranging from 358 J (machine limit) at 248 K

(–25 °C) to 100 to 200 J at 198 K (–75 °C). Reducing the Cu content to 0.94 wt pct showed an abrupt ductile-to-brittle transformation, but the measured lower shelf Charpy impact fracture energy was about 100 J at 198 K (–75 °C). These studies suggest an intriguing possibility of developing high-fracture energy steels for many applications, including possibly ductile hcp alloys and intermetallics, by using this concept.

## ACKNOWLEDGMENTS

This work was funded by the Infrastructure Technology Institute at Northwestern University, a national university transportation center, and by the Center for the Commercialization of Innovative Transportation Technology at Northwestern University, a university transportation center program of the Research and Innovative Technology Administration of the U.S. Department of Transportation, both through support from the Safe, Accountable, Flexible, Efficient Transportation Equity Act. Also, this work was funded by the National Science Foundation under Grant CCM1 0826535. Atom-probe tomography was performed at the Northwestern Center for Atom-Probe Tomography. The LEAP tomograph was purchased with funding from the National Science Foundation Major Research Instrumentation Program and the Office of Naval Research Defense University Research Instrumentation Program. One author (S.P.B.) acknowledges the encouragement and permission of ArcelorMittal Global R&D for this research work.

## REFERENCES

1. A.P. Coldren and T.B. Cox: *Technical report DTNSRDC/SME-CR-07-86*, David Taylor Research Laboratory, Bethesda, MD, 1986.
2. T.W. Montemarano, B.P. Sachs, J.P. Gudas, M.G. Vasilaros, and H.H. Vandervelt: *J. Ship Prod.*, 1986, vol. 3, pp. 145–62.
3. E.J. Czyricka, R.E. Link, J. Wong, D.A. Aylor, T.W. Montemarano, and J.P. Gudas: *Nav. Eng. J.*, 1990, vol. 102, pp. 63–82.
4. R.P. Foley: Ph.D. Dissertation, Northwestern University, Evanston, IL, 1992.
5. R.P. Foley and M.E. Fine: *Proc. Int. Conf. on Processing, Microstructure and Properties of Microalloyed and other Modern Low Alloy Steels*, ISS-AIME, Littleton, CO, 1991, pp. 315–30.
6. R.P. Foley and M.E. Fine: *Proc. Speich Symposium*, ISS-AIME, Littleton, CO, 1992, pp. 139–53.
7. R. Rana, S.B. Singh, W. Bleck, and O.N. Mohanty: *Metall. Mater. Trans. A*, 2009, vol. 40A, pp. 856–66.
8. C.S. Smith and E.W. Palmer: *Trans. AIME*, 1933, vol. 105, pp. 133–40.
9. S.K. Lahiri: Ph.D. Dissertation, Northwestern University, Evanston, IL, 1969.
10. S.K. Lahiri and M.E. Fine: *Metall. Trans.*, 1970, vol. 1, pp. 1495–99.
11. S.K. Lahiri, D. Chandra, L.H. Schwartz, and M.E. Fine: *Trans. Metall. Soc. AIME*, 1969, vol. 245, pp. 1865–68.
12. E. Hornbogen and R. C. Glen: *Trans. Metall. Soc. AIME*, 1960, vol. 218, p. 1064.
13. E. Hornbogen: *Trans. ASM*, 1964, vol. 57, p. 120.
14. A. Deschamps, M. Militzer, and W. J. Poole: *ISIJ Int.*, 2001, vol. 42, pp. 196–205.

15. S.R. Goodman, S.S. Brenner, and J.R. Low: *Metall. Trans.*, 1973, vol. 4, pp. 2363–69.
16. G.R. Speich, A.J. Schwoeble, and W.C. Leslie: *Metall. Trans.*, 1972, vol. 3, pp. 2031–37.
17. J. Weertman: *Phys. Rev.*, 1956, vol. 101, pp. 1429–30.
18. J. Weertman: *J Appl. Phys.*, 1958, vol. 29, pp. 1685–87.
19. W. Dickenscheid: Technical report AFML-TR-68-18, Universitaet Des Saarlandes Saarbruecken, Saarbruecken, Germany, 1968.
20. A. Urakami: Ph.D. Dissertation, Northwestern University, Evanston, IL, 1970.
21. A. Urakami and M.E. Fine: *Scripta Metall.*, 1970, vol. 4, pp. 667–72.
22. *Metals Handbook*, Volume 1, ASM International, Materials Park, OH, 1978, p. 691.
23. C. Zhang and M. Enmoto: *Acta Mater.*, 2006, vol. 54, pp. 4183–91.
24. G.R. Speich, A.J. Schwoeble, and W.C. Leslie: *Metall. Trans.*, 1972, vol. 3, pp. 2031–37.
25. S.W. Thompson and G. Krauss: *Metall. Mater. Trans. A*, 1996, vol. 27A, pp. 1573–84.